NANO LETTERS

pubs.acs.org/NanoLett Letter

Gate Controlled Excitonic Emission in Quantum Dot Thin Films

I K M Reaz Rahman, Shiekh Zia Uddin, Matthew Yeh, Naoki Higashitarumizu, Jongchan Kim, Quanwei Li, Hyeonjun Lee, Kyuho Lee, HoYeon Kim, Cheolmin Park, Jaehoon Lim, Joel W. Ager III, and Ali Javey*

Cite This: *Nano Lett.* 2023, 23, 10164–10170 Read Online

ACCESS | Metrics & More | Article Recommendations | Supporting Information

ABSTRACT: Formation of charged trions is detrimental to the luminescence quantum efficiency of colloidal quantum dot (QD) thin films as they predominantly undergo nonradiative recombination. In this regard, control of charged trion formation is of interest for both fundamental characterization of the quasi-particles and performance optimization. Using CdSe/CdS QDs as a prototypical material system, here we demonstrate a metal-oxide-semiconductor capacitor based on QD thin films for studying the background charge effect on the luminescence efficiency and lifetime. The concentration ratio of the charged and neutral quasiparticles in the QDs is reversibly controlled by applying a gate voltage, while simultaneous steady-state and time-resolved photoluminescence measurements are performed. Notably, the photoluminescence intensity is modulated by up to 2 orders of magnitude with a corresponding change in the effective lifetime. In addition, chip-scale modulation of brightness is demonstrated, where the photoluminescence is effectively turned on and off by the gate, highlighting potential applications in voltage-controlled electrochromics.

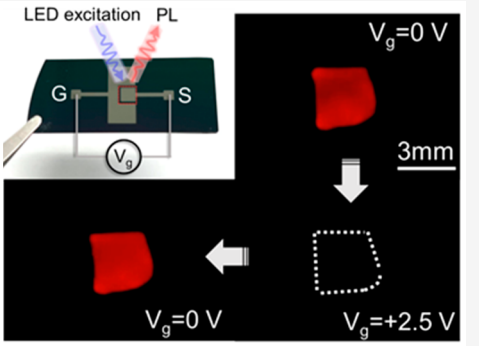

KEYWORDS: *quantum dot, exciton, trion, ionic gating, carrier lifetime*

Quantum dots (QD) have garnered substantial attention in the past decade as lighting and display technologies, quantum bits for quantum computation, and labels for biological systems.[1−6] Their diverse applications stem from a number of attractive properties such as size-tunable bandgap, narrow emission line width, high luminescence quantum yield, and host for single electron spin just to name a few.[7] The ease of fabrication with a solution-based process accounts for its prominence in optoelectronic applications like solid-state lighting, QD light emitting diodes (LEDs), and high optical gain lasers spanning multiple colors.[8−12] However, the advancement of QD electroluminescent devices has been impeded by performance degradation over time, predominantly attributed to charge accumulation or electric field-induced quenching. The effect of controlled charging was first explored by Galland et al. with spectroelectrochemistry on a single QD, leading to subsequent inquiries into the impact of charging within QD assemblies, wherein reduced photoluminescence was linked to nonradiative Auger processes triggered by charge imbalances.[13−16] In addition, the effect of a high electric field was also explored in a number of works where the authors demonstrated PL quenching induced by minimizing the spatial overlap of electron and hole wave function in the core of the QD through application of high electric field, also known as the quantum-confined Stark effect (QCSE). Subsequently, this lowers the radiative recombination in the QD film, resulting in a proportional decrease in PL.[4,17,18]

Light emitting devices employing QD film as the emissive layer suffer from the luminescence quantum yield diminishing with time due to charge accumulation or the quantum-confined Stark effect. Previous studies have not been able to disentangle the contributions of these two degradation mechanisms.[17,18] To suppress Auger recombination, alternative strategies emerged such as the design of core/graded-shell QDs and utilizing a thick shell to segregate the photogenerated excitons from the interface trap states of the dots.[14,19,20] The high electric field induced effect can be minimized through efficient design of charge transport layers, but even if this is done, it can be the case that a large fraction of QDs in an ensemble will still preserve a net residual charge due to imbalance in the injection mechanism.[21] For low-cost, efficient LEDs, it is imperative to explore the carrier recombination dynamics of both electron and hole charging. The effect of charge injection has been studied in the literature with electrochemical charging.[13,22,23] Another approach is to use a diode structure where charge carriers are injected into the emissive layer through electron and hole injection layers and

Received: July 2, 2023
Revised: November 2, 2023
Accepted: November 3, 2023
Published: November 7, 2023

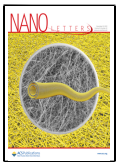

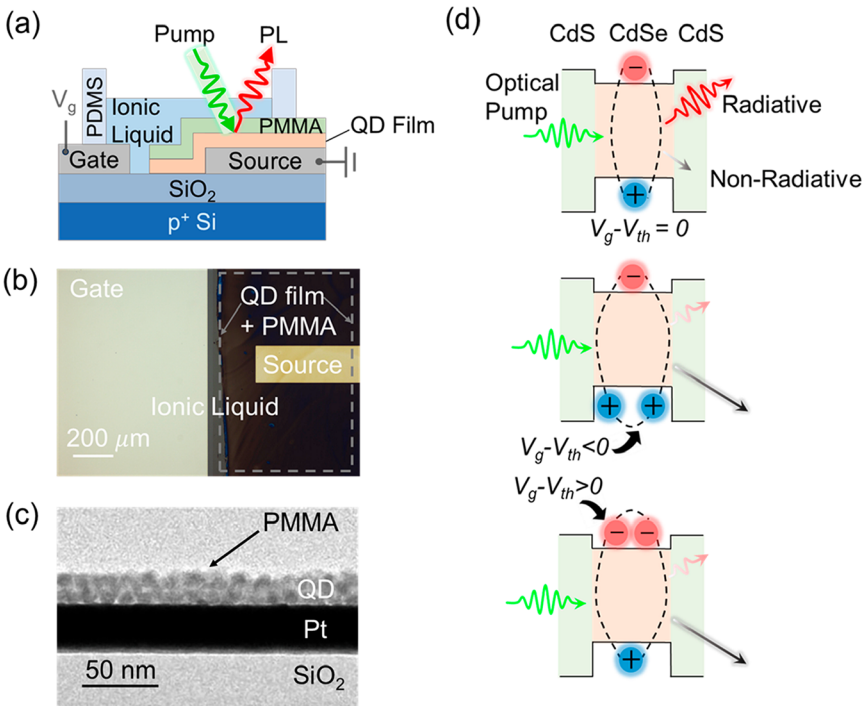

Figure 1. Charge injection in a quantum dot film. (a) Schematic cross-section of the device used to systematically study the recombination dynamics in thin film QD at various charging states. (b) Optical micrograph showing a uniform film of QD and PMMA over the source metal pad, using a dry patterning step. The spin-coated QD film area is highlighted by dashed lines. The ionic liquid, overlapping the entire field of view shown in the optical image, effectively applies the electric field across the QDs sitting on the source metal which is accommodated by injection of charge of relevant polarity. (c) TEM cross-section image along the source metal pad showing a very thin film of QDs on platinum. (d) Illustration of a core−shell CdSe/CdS QD with quasi type-II band alignment in (top to bottom) neutral, positive, and negatively charged states. In the neutral state, optical pumping creates excitons that mainly undergo radiative recombination. In the presence of an extra hole (electron), positive (negative) trions are formed which predominantly undergo nonradiative recombination as depicted by the length of the straight gray arrows.

the measurements are performed under continuous current flow.[14,24] For long-term reliable operation of thin-film QD light emitting devices, it is essential to develop QDs that are less sensitive to accumulated charge. In this regard, a test platform with facile fabrication steps that can probe the deterioration of thin film QDs with controlled charge injection is of interest and can serve as a rapid tool to characterize their robustness to charging.

In this work, we develop a platform to systematically study the separate effects of electron/hole injection in a QD ensemble, thereby probing their recombination dynamics with steady-state and time-resolved measurements. Inspired by the orders of magnitude modulation of luminescence intensity in monolayer transition metal dichalcogenides, we adopt a similar electrostatic approach to control background charge in nanoparticles through ionic liquid gating.[25−29] The same principle is extended to chip-scale modulation of the nanoparticle luminescence intensity, which is challenging to implement with a solid-state gate dielectric. The ability to reversibly control the luminescence intensity over a large area opens a new direction to utilize QD thin-film devices as voltage-tunable emitters in electrochromic applications such as optical downconversion.

The effect of charge injection into a thin QD film is investigated by applying a high electric field across a CdSe/CdS core−shell QD film using an ionic liquid gate (Figure 1a). The use of organic electrolyte based ionic liquid, which is molten salt at room temperature, as gate dielectric has gained considerable interest due to its ability to induce large carrier concentration in the active channel of a transistor.[30,31] By applying a potential to the ionic liquid with respect to the semiconductor (QDs), it is possible to create a redistribution of ions such that an electric double layer (EDL) is formed at the solid-electrolyte interface. Given the very short Debye length in ionic liquid and salt-based electrolytes, the applied voltage drops entirely across a few nanometers of EDL, resulting in a large gate capacitance that cannot be realized with a solid-state gate.[32,33] As a result, a large concentration of excess charge can accumulate on the QD ensemble, facilitated by the source metal pad. In addition, the ionic liquid is conformal, so issues that occur with pinholes in solid-state gate electrodes will not arise in ionic liquid gating. The QD emission area was defined by a dry patterning method using thin poly vinyl chloride as a mask, since the QD film is incompatible with wet lithography (see Supporting Information and Figure 1b). A cross-section transmission electron microscopy (TEM, Figure 1c) image of the device verifies that the dry patterning step can produce few layer QD film (e.g., two layers) without any residue. The chemical constituents of the various layers were confirmed with energy dispersive X-ray (EDX) mapping (Figure S1 and Table S1). A thin layer of poly(methyl methacrylate) (~5 nm) is used as an interlayer between the ionic liquid and QD film to prevent any redox reaction between the ligands of the QD and the ionic liquid within the electrochemical potential window of the electrolyte.[31,34]

We seek to measure the effect of different charging states in core−shell CdSe/CdS quantum dots on the radiative and nonradiative recombination rates, as shown schematically in Figure 1d. In the uncharged scenario, optical pumping with

https://doi.org/10.1021/acs.nanolett.3c02456
Nano Lett. 2023, 23, 10164−10170

above bandgap excitation leads to the formation of excitons within the core of the QD due to strong Coulombic interaction between the quasi particles. The result is dominant radiative recombination of excitons due to strong spatial overlap of the electron and hole wave function. Although some nonradiative processes could be present due to interface traps acting as hot carrier trapping sites as well as exciton dissociation close to a metal conductor, the overall recombination is dictated by radiative processes.[35] Using the analogy of a metal-oxide-semiconductor capacitor, for a negative gate bias below the threshold voltage (V_{th}), where V_{th} corresponds to the gate potential where the QDs are neutral, the resulting electric field leads to accumulation of holes in the QD assembly.[25] The excess hole promotes the formation of positive trions in the QD whose recombination is dominated by nonradiative decay. Similarly, a gate bias above the threshold voltage allows us to probe the recombination dynamics of negative trions formed by optical excitation in conjunction with electron injection.

First, we examined the relative rates by measuring the integrated PL counts of a charged ensemble of CdSe/CdS QDs as presented in Figure 2a. The QDs are charged by

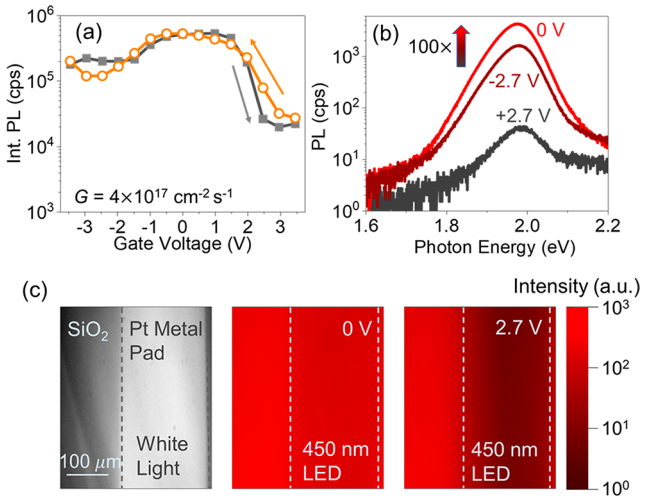

Figure 2. Modulation of photoluminescence intensity. (a) Integrated PL counts as a function of applied gate bias for CdSe/CdS QDs with an optical generation rate of 4×10^{17} cm^{-2} s^{-1}. A reversible change in PL can be observed while transitioning between the different charging states of the QD when the gate bias is swept in either direction. Orange (gray) arrow denotes the direction of the gate voltage sweep. (b) PL spectra of the QDs under different charging conditions as in (a). The corresponding gate biases are shown in the plot. (c) PL image of the QD ensemble under white light and above bandgap excitation from a 450 nm LED. When electrostatically gated, only the QDs over the metal pad undergo charging and demonstrate a modulation of PL intensity under optical pumping. The metal pad edges are shown by dashed lines in each plot along with the applied gate bias.

applying a dc gate bias to control the background charge concentration (N), which corresponds to the fraction of QDs that is charged in the ensemble. For steady-state measurement, this charge concentration can be estimated to a first-order approximation using a parallel plate capacitor model, as shown below.

$$N = C_{ox}(V_g - V_{th})/e \quad (1)$$

Here C_{ox} is the total gate capacitance of the system given by

$$\frac{1}{C_{ox}} = \frac{1}{C_{IL}} + \frac{1}{C_{PMMA}} \quad (2)$$

where $C_{IL} \approx 3.4$ μF cm^{-2} is the capacitance of the ionic liquid,[33] $C_{PMMA} \approx 0.25$ μF cm^{-2} is the capacitance of the polymer interlayer, and V_g is the applied gate bias and e is the electronic charge (see the Supporting Information). To determine V_{th} we consider the biasing regime where the ratio of radiative to nonradiative recombination rate is the highest. This is manifested by a higher PL count. As shown in Figure 2a, there is a plateau in the integrated PL counts as a function of gate voltage. We estimated the V_{th} to be 0.3 V by taking it as the middle of the plateau. Because V_{th} is slightly positive, the magnitude of the background charge concentration at a negative bias of −2.7 V (4.3×10^{12} cm^{-2}) is slightly larger than at a positive bias of 2.7 V (3.4×10^{12} cm^{-2}).

Due to the finite response time of the low mobility ions in the ionic liquid, the gate voltage was gradually ramped to the desired bias prior to the optical excitation of the QDs. There is more than one order change in PL counts transitioning between the bright (neutral exciton) and the dark (negative trion) states at positive gate voltages. The effect is less dramatic for positive trions at low negative gate voltages. As evidenced from Figure 2a, for a similar concentration of background electron or hole, there is an asymmetry in the PL counts that will be explained later. This process is fully reversible; the QDs retain their initial brightness even after multiple periods of charging−discharging cycle spanning 10s of minutes (Figure S2). It is to be noted that despite creating a large electric field across the QD film, the implemented device structure accommodates enhanced charge injection from the underlying metal pad and modulates the degree of charging only on the QDs overlapping the source electrode, as verified by PL imaging (Figure 2c). The absence of peak wavelength shift shows that the PL intensity modulation is not caused by QCSE (Figure 2b and Figure S3). The negligible gate leakage current within the relevant voltage range further corroborates the existence of excess charge residing within the thin film of QDs (Figure S4).

Next, we explore the evolution of the lifetime of the quasiparticles in the various charged states using time-resolved photoluminescence measurements. For the three regions of interest (neutral excitons, positive and negative trions), the PL decay of the QD nanoparticles is measured under pulsed excitation (Figure 3a). Here we note that, even without applying any bias to the QD film, we still see a multi-exponential decay due to the existence of a nonradiative recombination pathway by exciton quenching to the neighboring conductor surface. Therefore, we employ a biexponential model to fit the fast and slow component of the lifetime decay using the equation[36]

$$I(t) = A_{fast}e^{-t/\tau_{fast}} + A_{slow}e^{-t/\tau_{slow}} + B \quad (3)$$

where $A_{fast(slow)}$ is the amplitude weighting factor of the fast (slow) component of the decay, $\tau_{fast(slow)}$ is the fast (slow) effective lifetime, and B is the background count. During a decay cycle, a QD can be either in a charged state with formation of trions or uncharged while forming excitons. In an ensemble, the net occupation probabilities of the QDs in the charged and uncharged states must be unity. This is imposed by

$$A_{fast} + A_{slow} = 1 \quad (4)$$

https://doi.org/10.1021/acs.nanolett.3c02456
Nano Lett. 2023, 23, 10164−10170

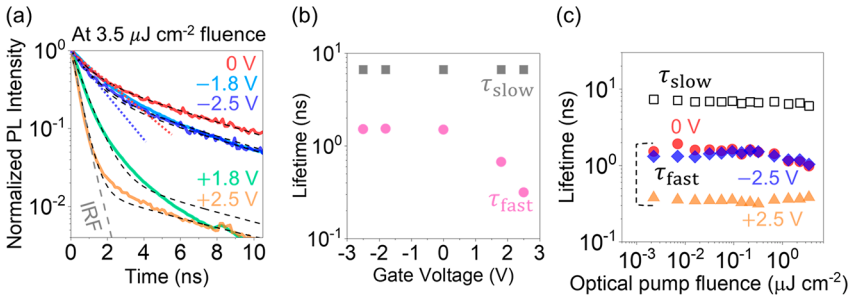

Figure 3. Time-resolved photoluminescence spectroscopy. (a) Lifetime decay trace for CdSe/CdS thin film QDs at different gate biases. All the decay curves show an initial fast decay component corresponding to nonradiative processes, followed by a slow decay pertinent to the radiative recombination of uncharged QDs. A biexponential model (black dashed lines) provides a reasonable fit to the fast lifetimes, keeping the slow decay component constant for all the charge states at any given fluence. The instrument response function (IRF) of the detector is shown in the same plot as dashed line. Note that at +2.5 V the fast decay component overlaps with the IRF, suggesting the measurement is limited by the IRF and the actual fast decay lifetime could be even shorter. The dotted lines are guide to the eye for the initial sharp decay. (b) Gate dependence of the lifetime at an optical fluence of 0.35 $\mu J\ cm^{-2}$. (c) Fast decay (solid marker) and slow decay lifetime (open marker) extracted from the biexponential fitting at various optical pump fluences (Table S2).

The fast decay component is dictated by several nonradiative channels including Auger recombination of trions, interface trap charge induced decay, and exciton dissociation to the metal surface, whereas the slow component is predominantly the radiative recombination lifetime of excitons in the uncharged state. As shown in Figure 3a, there are differences between the charged states concerning the initial fast decay. This is not the case for the slow decay at any given optical pump fluence. Therefore, using eqs 3 and 4, we perform a global fitting, keeping the slow lifetime fixed for a given pump fluence, while optimizing the amplitude weighting factor and the fast lifetime. This enables us to extract the individual fast lifetimes corresponding to the different charged states and the common slow lifetime for any given optical pump fluence (Figure 3b and Table S2 in Supporting Information). Positive trions in CdSe/CdS QDs have been shown to have a shorter nonradiative lifetime than negative trions due to strong localized hole wave function in the core of the QD.[37,38] However, we observe a slow decay profile for positive trions with a negative gate bias. It should be noted that eq 1 assumes the contact to the QDs is able to provide the charge demanded by the gate voltage. Given the rather large barrier height for hole injection in CdSe/CdS QDs,[39] eq 1 may in fact overestimate the value for N with applied negative gate bias. Thus, the observed asymmetry in PL counts versus gate voltage in Figure 2a may partly be attributed to the energy barrier height of the contacts in addition to the differences of the lifetimes for negative and positive trions. The QD film undergoes significant charging from electron injection, which translates into more than an order of magnitude change in integrated PL counts, as supported by the stark difference in the fast and slow components of the lifetime decay at +2.5 V (Figure 3c). Once the negative trions undergo fast nonradiative recombination on the time scale of 100s of picoseconds, the remaining uncharged QDs then radiatively recombine with their slow lifetime being exhibited in the decay profile. Note that at +2.5 V the fast decay component overlaps with the instrument response function (IRF), suggesting that the measurement was limited by the IRF and the actual fast decay lifetime could be even shorter. For the range of optical pump fluence studied, the different components of the lifetime remain constant, indicating the absence of biexcitons (Figure S5).[25,40]

The versatility of ionic liquid gating complemented with uniform close packing of nanocrystals from solution-processed films inspired us to demonstrate a millimeter-scale luminescent film whose brightness can be reversibly tuned by controlled charge injection (Figure 4). As the gate bias is gradually

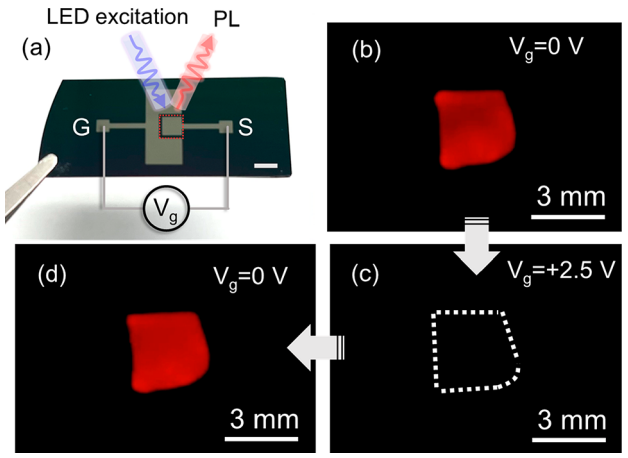

Figure 4. Reversible modulation of PL intensity in large area luminescent film. (a) Optical image of the millimeter scale device along with schematic diagram showing how the gate bias is applied and the film is optically pumped. The QD film over the large source pad is highlighted by dotted lines. Scale bar: 3 mm. (b–d) Snapshots from recorded video, showing reversible modulation of brightness at initial (0 V), charged (+2.5 V), and discharged states (0 V again). The corresponding applied gate biases are also shown in the plot. At 2.5 V, the dramatic change in PL intensity can be readily observed by eye in the video as the QD film becomes dimmer and reaches similar intensity as background. The dotted lines highlight the luminescent area in the dark state.

ramped to charge the QD ensemble with electrons, the PL intensity of the nanocrystal film drops by 2 orders of magnitude, which is apparent from the complete dimming of PL in the luminescent film area. Reversible modulation of brightness is achieved by discharging the film with a gate potential of equal magnitude but opposite in sign (supplementary video). This highlights the promise of voltage tunable phosphor with emission in the near-infrared regime and beyond.

https://doi.org/10.1021/acs.nanolett.3c02456
Nano Lett. 2023, 23, 10164−10170

In summary, we have demonstrated a platform for the controlled injection of charge in an assembly of QDs that allows us to investigate the deterioration of luminescent devices with charge accumulation. The polarity of gate bias enables us to selectively probe the different charging states in the QD film in terms of the transient quasiparticle lifetime that is dictated by the various recombination channels in the system. The resulting modulation of PL is found to be dependent on the fast nonradiative recombination lifetime of the charged nanoparticles and the degree of charging in the ensemble. With the feasibility of large-scale operation, the device structure can be applied as a bias-dependent phosphor across a wide range of emission wavelengths.

■ ASSOCIATED CONTENT

Supporting Information

The Supporting Information is available free of charge at https://pubs.acs.org/doi/10.1021/acs.nanolett.3c02456.

Methods, energy dispersive X-ray analysis of the chemical constituents in the device cross-section, extended period of charging−discharging QD film, normalized PL spectra under charge injection, gate current through ionic liquid, time-resolved PL and lifetime of the CdSe/CdS QDs under different optical pump fluence and gate bias, tables of elemental weight-percentage and atomic-percentages from EDX and components of lifetime decay (PDF)

Reversible modulation of brightness in chip-scale luminescent QD film (MP4)

■ AUTHOR INFORMATION

Corresponding Author

Ali Javey − *Electrical Engineering and Computer Sciences, University of California, Berkeley, California 94720, United States; Materials Sciences Division, Lawrence Berkeley National Laboratory, Berkeley, California 94720, United States;* orcid.org/0000-0001-7214-7931; Email: ajavey@berkeley.edu

Authors

I K M Reaz Rahman − *Electrical Engineering and Computer Sciences, University of California, Berkeley, California 94720, United States; Materials Sciences Division, Lawrence Berkeley National Laboratory, Berkeley, California 94720, United States;* orcid.org/0000-0003-3911-4681

Shiekh Zia Uddin − *Electrical Engineering and Computer Sciences, University of California, Berkeley, California 94720, United States; Materials Sciences Division, Lawrence Berkeley National Laboratory, Berkeley, California 94720, United States;* Present Address: Department of Physics, Massachusetts Institute of Technology, Cambridge, MA 02139, USA

Matthew Yeh − *Electrical Engineering and Computer Sciences, University of California, Berkeley, California 94720, United States; Materials Sciences Division, Lawrence Berkeley National Laboratory, Berkeley, California 94720, United States;* Present Address: John A. Paulson School of Engineering and Applied Sciences, Harvard University, Cambridge, MA 02138, USA

Naoki Higashitarumizu − *Electrical Engineering and Computer Sciences, University of California, Berkeley, California 94720, United States; Materials Sciences Division, Lawrence Berkeley National Laboratory, Berkeley, California 94720, United States;* orcid.org/0000-0003-3996-6753

Jongchan Kim − *Electrical Engineering and Computer Sciences, University of California, Berkeley, California 94720, United States; Materials Sciences Division, Lawrence Berkeley National Laboratory, Berkeley, California 94720, United States;* Present Address: Department of Integrated Display Engineering, Yonsei University, Seoul, 120-749, Republic of Korea; orcid.org/0000-0003-3005-9268

Quanwei Li − *Department of Chemistry, University of California, Berkeley, California 94720, United States; Kavli Energy Nanoscience Institute at Berkeley, Berkeley, California 94720, United States*

Hyeonjun Lee − *Department of Energy Science and Centre for Artificial Atoms, Sungkyunkwan University, Suwon 16419 Gyeonggi-do, Republic of Korea;* orcid.org/0000-0003-0616-8122

Kyuho Lee − *Electrical Engineering and Computer Sciences, University of California, Berkeley, California 94720, United States; Materials Sciences Division, Lawrence Berkeley National Laboratory, Berkeley, California 94720, United States; Materials Science and Engineering, Yonsei University, Seoul 03722, Republic of Korea*

HoYeon Kim − *Materials Science and Engineering, Yonsei University, Seoul 03722, Republic of Korea*

Cheolmin Park − *Materials Science and Engineering, Yonsei University, Seoul 03722, Republic of Korea;* orcid.org/0000-0002-6832-0284

Jaehoon Lim − *Department of Energy Science and Centre for Artificial Atoms, Sungkyunkwan University, Suwon 16419 Gyeonggi-do, Republic of Korea;* orcid.org/0000-0003-2623-3550

Joel W. Ager III − *Materials Sciences Division, Lawrence Berkeley National Laboratory, Berkeley, California 94720, United States; Materials Science and Engineering, University of California, Berkeley, California 94720, United States;* orcid.org/0000-0001-9334-9751

Complete contact information is available at: https://pubs.acs.org/10.1021/acs.nanolett.3c02456

Author Contributions

R.R., S.Z.U., and A.J. conceived the idea for the project and designed the experiments. H.L and J.L synthesized quantum dots. R.R., S.Z.U., M.Y., N.H., J.K., Q.L. and J.W.A. fabricated devices and performed optical measurements. R.R., K.L., and H.K. performed the optical imaging. R.R., N.H., and A.J. analyzed the data and wrote the manuscript. All authors discussed the results and commented on the manuscript.

Notes

The authors declare no competing financial interest.

■ ACKNOWLEDGMENTS

This work was funded by the U.S. Department of Energy, Office of Science, Office of Basic Energy Sciences, Materials Sciences and Engineering Division under Contract No. DE-AC02-05-CH11231 (EMAT program KC1201). Work at the Molecular Foundry was supported by the Office of Science, Office of Basic Energy Sciences, of the U.S. Department of Energy under Contract No. DE-AC02-05CH11231. The device fabrication part of this work was funded by Samsung Display. N.H. acknowledges support from Postdoctoral Fellowships for Research Abroad of the Japan Society for the

Promotion of Science. The authors acknowledge A. Paul Alivisatos for stimulating discussions and Shogo Tajima for his support in device fabrication.

REFERENCES

(1) Shirasaki, Y.; Supran, G. J.; Bawendi, M. G.; Bulovic, V. Colloidal QDs for Light-Emitting Applications. *Nat Photonics* **2013**, *7* (1), 13−23.
(2) Dai, X.; Deng, Y.; Peng, X.; Jin, Y.; Dai, X.; Deng, Y.; Jin, Y.; Peng, X. Quantum-Dot Light-Emitting Diodes for Large-Area Displays: Towards the Dawn of Commercialization. *Adv. Mater.* **2017**, *29* (14), No. 1607022.
(3) Martynenko, I. V; Litvin, A. P.; Purcell-Milton, F.; Baranov, A. V; Fedorov, A. V; Gun'ko, Y. K. Application of Semiconductor Quantum Dots in Bioimaging and Biosensing. *J. Mater. Chem. B* **2017**, *5*, 6701.
(4) Rowland, C. E.; Susumu, K.; Stewart, M. H.; Oh, E.; Mä Kinen, A. J.; O'shaughnessy, T. J.; Kushto, G.; Wolak, M. A.; Erickson, J. S.; Efros, A. L.; Huston, A. L.; Delehanty, J. B. Electric Field Modulation of Semiconductor Quantum Dot Photoluminescence: Insights Into the Design of Robust Voltage-Sensitive Cellular Imaging Probes. *Nano Lett* **2015**, *15* (10), 6848−6854.
(5) Kagan, C. R.; Bassett, L. C.; Murray, C. B.; Thompson, S. M. Colloidal Quantum Dots as Platforms for Quantum Information Science. *Chem Rev* **2021**, *121* (5), 3186−3233.
(6) Harankahage, D.; Cassidy, J.; Yang, M.; Porotnikov, D.; Williams, M.; Kholmicheva, N.; Zamkov, M. Quantum Computing with Exciton Qubits in Colloidal Semiconductor Nanocrystals. *J. Phys. Chem. C* **2021**, *125*, 22195−22203.
(7) Kagan, C. R.; Lifshitz, E.; Sargent, E. H.; Talapin, D. V. Building Devices from Colloidal Quantum Dots. *Science (1979)* **2016**, *353* (6302), aac5523.
(8) Yang, X.; Mutlugun, E.; Dang, C.; Dev, K.; Gao, Y.; Tiam Tan, S.; Wei Sun, X.; Volkan Demir, H. Highly Flexible, Electrically Driven, Top-Emitting, Quantum Dot Light-Emitting Stickers. *ACS Nano* **2014**, *8* (8), 8224−8231.
(9) Kwak, J.; Bae, W. K.; Lee, D.; Park, I.; Lim, J.; Park, M.; Cho, H.; Woo, H.; Yoon, D. Y.; Char, K.; Lee, S.; Lee, C. Bright and Efficient Full-Color Colloidal Quantum Dot Light-Emitting Diodes Using an Inverted Device Structure. *Nano Lett* **2012**, *12* (5), 2362−2366.
(10) Dai, X.; Zhang, Z.; Jin, Y.; Niu, Y.; Cao, H.; Liang, X.; Chen, L.; Wang, J.; Peng, X. Solution-Processed, High-Performance Light-Emitting Diodes Based on Quantum Dots. *Nature* **2014**, *515*, 96−99.
(11) Dang, C.; Lee, J.; Breen, C.; Steckel, J. S.; Coe-Sullivan, S.; Nurmikko, A. Red, Green and Blue Lasing Enabled by Single-Exciton Gain in Colloidal Quantum Dot Films. *Nat Nanotechnol* **2012**, *7* (5), 335−339.
(12) Park, Y.-S.; Roh, J.; Diroll, B. T.; Schaller, R. D.; Klimov, V. I. Colloidal Quantum Dot Lasers. *Nat Rev Mater* **2021**, *6* (5), 382−401.
(13) Galland, C.; Ghosh, Y.; Steinbrück, A.; Sykora, M.; Hollingsworth, J. A.; Klimov, V. I.; Htoon, H. Two Types of Luminescence Blinking Revealed by Spectroelectrochemistry of Single Quantum Dots. *Nature* **2011**, *479*, 203.
(14) Bae, W. K.; Park, Y.-S.; Lim, J.; Lee, D.; Padilha, L. A.; Mcdaniel, H.; Robel, I.; Lee, C.; Pietryga, J. M.; Klimov, V. I. Controlling the Influence of Auger Recombination on the Performance of Quantum-Dot Light-Emitting Diodes. *Nat Commun* **2013**, *4* (1), 2661.
(15) Keating, L. P.; Lee, H.; Rogers, S. P.; Huang, C.; Shim, M. Charging and Charged Species in Quantum Dot Light-Emitting Diodes. *Nano Lett* **2022**, *22* (23), 9500−9506.
(16) Shendre, S.; Sharma, V. K.; Dang, C.; Demir, H. V. Exciton Dynamics in Colloidal Quantum-Dot LEDs under Active Device Operations. *ACS Photonics* **2018**, *5*, 480−486.
(17) Xie, S.; Zhu, H.; Li, M.; Bulovic, V. Voltage-Controlled Reversible Modulation of Colloidal Quantum Dot Thin Film Photoluminescence. *Appl. Phys. Lett.* **2022**, *120* (21), No. 211104.
(18) Bozyigit, D.; Yarema, O.; Wood, V. Origins of Low Quantum Efficiencies in Quantum Dot LEDs. *Adv Funct Mater* **2013**, *23* (24), 3024−3029.
(19) Bae, W. K.; Padilha, L. A.; Park, Y.-S.; McDaniel, H.; Robel, I.; Pietryga, J. M.; Klimov, V. I. Controlled Alloying of the Core-Shell Interface in CdSe/CdS Quantum Dots for Suppression of Auger Recombination. *ACS Nano* **2013**, *7* (4), 3411−3419.
(20) Lee, T.; Kim, B. J.; Lee, H.; Hahm, D.; Bae, W. K.; Lim, J.; Kwak, J. Bright and Stable Quantum Dot Light-Emitting Diodes. *Adv. Mater.* **2022**, *34* (4), No. 2106276.
(21) Zhu, X.; Liu, Y.; Liu, H.; Li, X.; Ni, H.; Tao, H.; Zou, J.; Xu, M.; Wang, L.; Peng, J.; Cao, Y. Optimization of Carrier Transport Layer: A Simple but Effective Approach toward Achieving High Efficiency All-Solution Processed InP Quantum Dot Light Emitting Diodes. *Org Electron* **2021**, *96*, 106256.
(22) Morozov, S.; Pensa, E. L.; Khan, A. H.; Polovitsyn, A.; Cortés, E.; Maier, S. A.; Vezzoli, S.; Moreels, I.; Sapienza, R. Electrical Control of Single-Photon Emission in Highly Charged Individual Colloidal Quantum Dots. *Sci. Adv.* **2020**, *6* (38), abb1821.
(23) Park, J.; Won, Y. H.; Kim, T.; Jang, E.; Kim, D. Electrochemical Charging Effect on the Optical Properties of InP/ZnSe/ZnS Quantum Dots. *Small* **2020**, *16* (41), 2003542.
(24) Shendre, S.; Sharma, V. K.; Dang, C.; Demir, H. V. Exciton Dynamics in Colloidal Quantum-Dot LEDs under Active Device Operations. *ACS Photonics* **2018**, *5*, 480−486.
(25) Lien, D.-H.; Uddin, S. Z.; Yeh, M.; Amani, M.; Kim, H.; Ager, J. W.; Yablonovitch, E.; Javey, A. Electrical Suppression of All Nonradiative Recombination Pathways in Monolayer Semiconductors. *Science (1979)* **2019**, *364* (6439), 468−471.
(26) Kim, H.; Uddin, S. Z.; Higashitarumizu, N.; Rabani, E.; Javey, A. Inhibited Nonradiative Decay at All Exciton Densities in Monolayer Semiconductors. *Science (1979)* **2021**, *373* (6553), 448−452.
(27) Uddin, S. Z.; Higashitarumizu, N.; Kim, H.; Rahman, I. K. M. R.; Javey, A. Efficiency Roll-Off Free Electroluminescence from Monolayer WSe2. *Nano Lett* **2022**, *22* (13), 5316−5321.
(28) Uddin, S. Z.; Higashitarumizu, N.; Kim, H.; Rabani, E.; Javey, A. Engineering Exciton Recombination Pathways in Bilayer WSe2 for Bright Luminescence. *ACS Nano* **2022**, *16*, 1339−1345.
(29) Uddin, S. Z.; Higashitarumizu, N.; Kim, H.; Yi, J.; Zhang, X.; Chrzan, D.; Javey, A. Enhanced Neutral Exciton Diffusion in Monolayer WS 2 by Exciton−Exciton Annihilation. *ACS Nano* **2022**, *16*, 8005−8011.
(30) Fujimoto, T.; Awaga, K. Electric-Double-Layer Field-Effect Transistors with Ionic Liquids. *Phys. Chem. Chem. Phys.* **2013**, *15*, 8983.
(31) Yuan, H.; Shimotani, H.; Tsukazaki, A.; Ohtomo, A.; Kawasaki, M.; Iwasa, Y. High-Density Carrier Accumulation in ZnO Field-Effect Transistors Gated by Electric Double Layers of Ionic Liquids. *Adv Funct Mater* **2009**, *19* (7), 1046−1053.
(32) Smith, A. M.; Lee, A. A.; Perkin, S. The Electrostatic Screening Length in Concentrated Electrolytes Increases with Concentration. *J Phys Chem Lett* **2016**, *7* (12), 2157−2163.
(33) Thiemann, S.; Sachnov, S.; Porscha, S.; Wasserscheid, P.; Zaumseil, J. Ionic Liquids for Electrolyte-Gating of ZnO Field-Effect Transistors. *The Journal of Physical Chemistry C* **2012**, *116* (25), 13536−13544.
(34) Misra, R.; McCarthy, M.; Hebard, A. F. Electric Field Gating with Ionic Liquids. *Appl. Phys. Lett.* **2007**, *90*, 52905.
(35) Kagan, C. R.; Murray, C. B.; Bawendi, M. G. Long-Range Resonance Transfer of Electronic Excitations in Close-Packed CdSe Quantum-Dot Solids. *Phys Rev B* **1996**, *54* (12), 8633.
(36) Deng, Y.; Lin, X.; Fang, W.; Di, D.; Wang, L.; Friend, R. H.; Peng, X.; Jin, Y. Deciphering Exciton-Generation Processes in Quantum-Dot Electroluminescence. *Nat Commun* **2020**, *11* (1), 2309.
(37) Wu, K.; Lim, J.; Klimov, V. I. Superposition Principle in Auger Recombination of Charged and Neutral Multicarrier States in Semiconductor Quantum Dots. *ACS Nano* **2017**, *11* (8), 8437−8447.

https://doi.org/10.1021/acs.nanolett.3c02456
Nano Lett. 2023, 23, 10164−10170

(38) Xu, W.; Hou, X.; Meng, Y.; Meng, R.; Wang, Z.; Qin, H.; Peng, X.; Chen, X.-W. Deciphering Charging Status, Absolute Quantum Efficiency, and Absorption Cross Section of Multicarrier States in Single Colloidal Quantum Dots. *Nano Lett* **2017**, *17* (12), 7487−7493.
(39) Cao, W.; Xiang, C.; Yang, Y.; Chen, Q.; Chen, L.; Yan, X.; Qian, L. Highly Stable QLEDs with Improved Hole Injection via Quantum Dot Structure Tailoring. *Nat. Commun.* **2018**, *9*, 2068.
(40) Amani, M.; Lien, D. H.; Kiriya, D.; Xiao, J.; Azcatl, A.; Noh, J.; Madhvapathy, S. R.; Addou, R.; Santosh, K. C.; Dubey, M.; Cho, K.; Wallace, R. M.; Lee, S. C.; He, J. H.; Ager, J. W.; Zhang, X.; Yablonovitch, E.; Javey, A. Near-Unity Photoluminescence Quantum Yield in MoS2. *Science (1979)* **2015**, *350* (6264), 1065−1068.

https://doi.org/10.1021/acs.nanolett.3c02456
Nano Lett. 2023, 23, 10164−10170